Journal of Mining and Environment (JME) Vol. 12, No. 3, 2021, 769-783

Shahrood University of Technology

Iranian Society of Mining Engineering (IRSME)

Journal of Mining and Environment (JME)

journal homepage: www.jme.shahroodut.ac.ir

THOMSON REUTERS

Compressive Failure Analyses of Rock-Like Materials by Experimental and Numerical Methods

Mohammad Davood Yavari[1], Hadi Haeri[2], Vahab Sarfarazi[3], Mohammad Fatehi Marji[4]* and Hossein Ali Lazemi[1]

1. Department of Mining Engineering, Bafgh Branch, Islamic Azad University, Bafgh, Iran
2. State Key Laboratory for Deep GeoMechanics and Underground Engineering, Beijing, China
3. Department of Mining Engineering, Hamedan University of Technology, Hamedan, Iran
4. Mine Exploitation Engineering Department, Faculty of Mining and Metallurgy, University of Yazd, Yazd, Iran

Article Info

Received 9 May 2021
Received in Revised form 29 May 2021
Accepted 03 June 2021
Published online 03 June 2021

DOI:10.22044/jme.2021.10819.2052

Keywords

Cracking mechanism
Fracture mechanics
Cubic specimen
Physical modeling
FEM

Abstract

Investigating the crack propagation mechanism is of paramount importance in analyzing the failure process of most materials. This process may be exposed during each kind of loading on the materials. In this work, the cracking mechanism in rock-like materials is studied using the numerical methods and compared with the experimental test results. However, the mechanism of crack growth in brittle materials such as rocks is influenced by different parameters. This research work focuses on the effect of the initial crack angles on the crack growth paths of these materials. Some cubic samples containing pre-existing cracks are tested in compression by considering different flaw orientations. The specimens are made of cement, water, and sand. Moreover, the mentioned process is numerically simulated using three different methods: the finite difference method for discontinuous bodies or discrete element method, the displacement discontinuity method, and the versatile finite element method. The micro-parameters for simulation are gained by the trial-and-error procedure for the discrete element method. Eventually, the crack growth paths observed in the experiments are compared with the numerically simulated models. The results obtained show that these central cracks propagate in two ways, which are dependent on their initial angle. By increasing the initial crack angle to greater than 30° ($\alpha > 30°$), the wing crack path moves further away from the initial crack, and by decreasing α to smaller than 30° ($\alpha < 30°$), only the shear cracks are initiated. Therefore, the validity and accuracy of the results are manifested by comparing all the corresponding results obtained by different methods. Based on these results, it can generally be concluded that the strength of the cubic (rock material) specimens increases with increase in the crack angles with respect to the applied loading direction.

1. Introduction

Some brittle materials consisting of the civil and rock structures have various micro-cracks in their constructions. Based on the Griffith theory, new fractures can be created from the extension of the pre-existing cracks in the concretes and rocks. For example, in rock-like material specimens, the pre-existing cracks mainly propagate in two manners under compression, i.e. the tensile (wing) cracks propagate first, and then the shear (secondary) cracks are extended. Specifically, the tensile cracks

Corresponding author: mohammad.fatehi@gmail.com (M. Fatehi Marji).

start their propagation first, and continue their extension from the tip of the pre-existing cracks, and then the shear cracks start their initiation near the crack tip but continue to propagate in the direction of the maximum shear stress [1-4]. Thus the wing cracks may occur more possible than the secondary cracks in rock-like materials because the Mode I (tensile mode) fracture toughness of the specimens is lower than the toughness in shear loading. Therefore, it is significant to investigate the failure mechanism of wing and secondary cracks of brittle materials [1]. Already, several analytical, experimental, and numerical studies have been accomplished on the fracture mechanics and crack propagation process of rock-like materials [5-8].

However, several experimental works have been performed considering the mechanism of crack extensions in brittle material samples containing one or more cracks, and some valuable laboratory results have been provided in the literature. For example, the mechanism of crack growth and coalescence in three-dimensions for the rock-like material samples with a spherical pore [9-11] and two pre-existing cracks [12] have been experimentally studied under biaxial [13] and tri-axial [14] compression. The fracture mechanics of the rock-like material samples with pre-existing cracks under compression have been studied by several researchers [15-18]. On the other hand, in [19-22], some experiments have been carried out in order to investigate the distribution of the fractures in the rock-like samples under compression loading. The interaction between the pre-existing holes in the geo-materials under uniaxial compression test has been studied [23, 24]. Also some uniaxial tests have been performed in order to investigate the fracturing mechanism and failure behavior of the rock-like material samples with a large-opening crack [14]. Moreover, Sun et al. [25] have investigated the interaction between the central and edge cracks in the specimens of rock-like materials.

In addition to the experimental studies, several types of research works have focused on the fracture mechanics, process of cracks extension, and crack coalescence in the geo-materials specimens using the numerical and experimental-numerical methods [26]. For example, the crack propagation process between the cracks and holes in the specimens of rock-like material under uniaxial compression has been studied using the Discrete Element Method (DEM) [14, 23, 24, 27-29]. Moreover, a Boundary-Finite Element Method (BEM-FEM) has been presented for modeling the wing crack propagation in the pre-existing crack problems [30]. Crack growth from a spherical pore in brittle materials has been simulated by the Finite Element Method (FEM) [11, 15]. Some crack growth simulations in geo-materials have been performed using the particle flow codes (PFCs) in two and three dimensions [31, 32].

In addition to the static problems, there are some quasi-static and dynamic research works in the literature considering the dynamic crack growth mechanism in brittle geo-materials. These works have mainly focused on the dynamic crack propagation in rock specimens due to the Hopkinson pressure test [14, 33, 34] and the numerical dynamic loadings [35, 36]. Moreover, dynamic crack growth due to rock blasting has also been investigated using both the numerical analyses and experimental tests [37-40].

Therefore, the solutions to the rock fracture mechanics problems related to the initiation, propagation, extension paths of the pre-existing cracks in geo-materials are important from the theoretical and practical viewpoint for many engineers dealing with the surface and underground rock structures. Most of the previous studies have focused on a special problem with specific crack geometry and specific material properties using one or two methods. In this research work, the cubic type of rock-like materials containing cracks are specially prepared in the laboratory and tested under compressive loading. The mechanism of crack growth paths is investigated. The observed experimental results showing the formation of the wing and secondary cracks are compared with the modeled results obtained using FEM, BEM, and DEM. Various types of specimens considering different crack inclination angles are studied in this research work. The process of rock fracturing for different scenarios are considered, and the corresponding results of each method are compared with one another, which provide the validity and accuracy of these different results.

2. Experimentally observed crack growth mechanism for rock-like specimens

In this work, the physical modeling and laboratory tests were conducted in order to experimentally analyze the mechanism of the crack growth process in brittle materials. The cube specimens were provided by mixing 15% of Portland Pozzolana cement (PPC), 75% of fine sands, and 10% water, and dried at room temperature. The specimen dimensions were 15 ×

15 × 15 cm. Then the propagation mechanism of the wing and shear (secondary) cracks initiating from the tips of a central slant crack were studied experimentally by carrying out several laboratory tests. A schematic view of the prepared specimen with a central slant crack and the orientation angle (α) is shown in Figure 1. Five specimens with slant cracks of α = 0°, 15°, 30°, 45°, and 55° were constructed as shown in Figures 2(a) to 2(e).

The uniaxial compression tests were carried out on the cubic specimens prepared from the concrete materials (Figure 3). In these tests, a constant loading rate of 0.02 MPa/s was uniformly applied on the cubic type pre-cracked specimens.

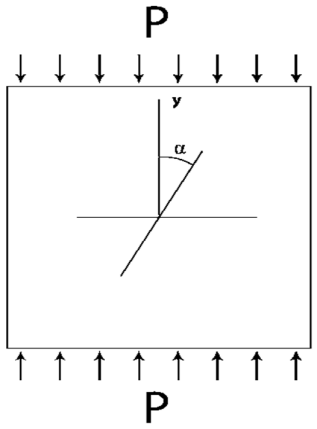

Figure 1: A schematic view of the setup of specimens.

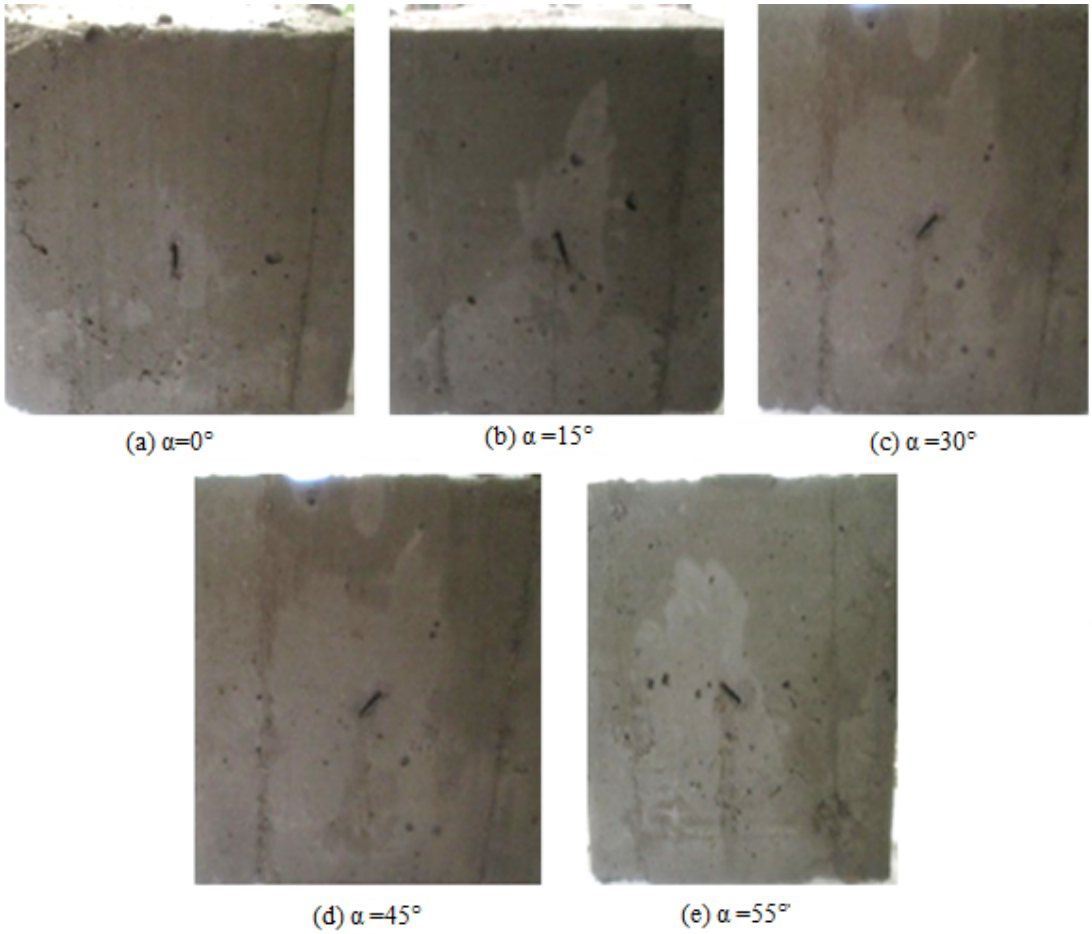

Figure 2: Constructed specimens with a central crack considering different crack inclination angles.

Figure 3: Uniaxial compression test system.

3. Numerical modeling of crack propagation

In this section, in the physical modelling stage, the specimens were constructed and tested in the laboratory. Then in the numerical simulation stage, they were numerically simulated using: i) a quadratic element displacement discontinuity code (TDDQCR), which was a modified indirect boundary element method (BEM) [40-42], ii) the well-known Abaqus software (based on FEM), iii) the particle flow code (PFC) (based on DEM). The main geometrical and mechanical properties of the rock-like materials used in the modelled specimens is given in Table 1. Eventually, the crack propagation paths obtained from the experiments were compared with the corresponding numerical models.

Table 1: Rock-like material parameters used in numerical modeling of the modelled specimens.

Parameter	Value
Crack length (mm)	10
Fracture toughness (MPa√m)	0.23
Elastic modulus (GPa)	10
Poisson ratio	0.2
Crack tip length (mm)	0.177
Cohesion (MPa)	5

3.1. Boundary element modeling of problem

The direct and indirect boundary element methods (BEMs) were developed in 1970s for the numerical analyses of many boundary value problems in engineering and science [43-45]. Recently, the higher order elements have been used in order to solve many rock fracture problems. In the semi-analytical BEM, the problem boundaries are discretized into a finite number of boundary elements. In the analytical part of the solution, the potential variables such as the displacement and traction vectors are specified to the nodes of these elements in the form of boundary integral equations (BIEs). Then a set of simultaneous algebraic equations are numerically arranged relating the solved boundary integral equations to one another. Using the proper boundary conditions (and the initial conditions for dynamic problems), the tractions, displacements or intermediate unknown variables such as fictitious stresses or displacement discontinuities at all boundary nodes are obtained as the numerical solution of these algebraic equations [41]. In the modified form of DDM, i.e. the higher order displacement discontinuity method (HODDM), some higher order displacement discontinuity (HDD) elements are specified to each boundary element and/or crack element. This code is specially modified to solve the 2D fracture mechanics problems [42-44].

In this section, the modified form of the displacement discontinuity (DD) method [45] is used for crack analyses. The higher order quadratic DD elements and the special crack tip elements are specified at the boundaries and crack tips, respectively. This computer code is known as the Two-dimensional Displacement Discontinuity method using Quadratic elements for Crack analyses (TDDQCR). The crack extension process in rock-like specimens is simulated by the proposed method [10, 46-49].

Figure 4a shows the 2D displacement discontinuity distribution at quadratic collocation point *m*. The quadratic displacement discontinuity variations along the boundary elements can be expressed as:

$$D_j(\xi) = \sum A_m(\xi)\, D_j^m \qquad (1)$$

($j=x,y;\ m=1,2,3$)

where D_j^1, D_j^2, and D_j^3 are the nodal shear and normal displacement discontinuities at the j^{th} element in the x and y directions. How to determine these parameters and the shape functions of DDM has already been explained in [26].

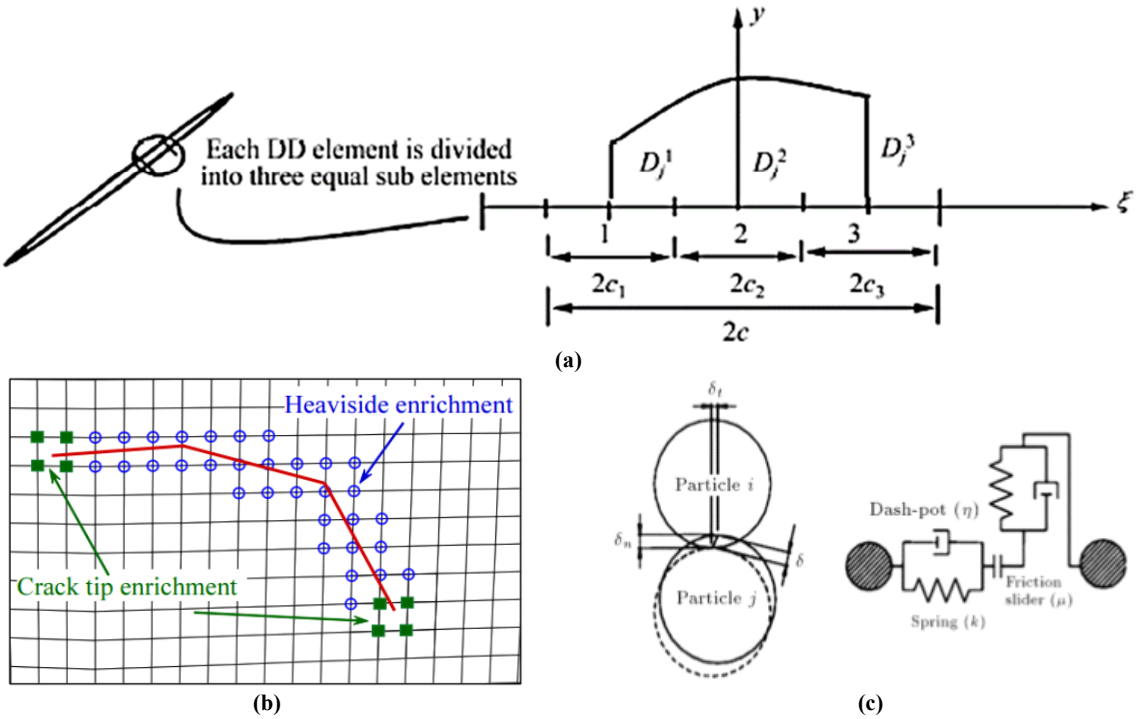

Figure 4: Discretizing each boundary element into a quadratic element to specify its displacement discontinuities [26], b) Enriched nodes in XFEM [53], c) contact for a PFC model [60].

In the TDDQCR code, the crack tip singularity effects of the displacement discontinuities can be minimized by providing some accurate estimations of the stress distribution near the crack ends. This procedure increases the accuracy of the displacement discontinuity components. However, a special treatment of the crack (at its tip only) has been used in this computer code [26, 50]. On the other hand, the Mode I and Mode II (mixed mode) stress intensity factors (denoted as K_I and K_{II}) have been numerically estimated based on the famous concepts of crack opening displacement (COD) and crack sliding displacement (CSD), respectively. In this approach, COD and CSD represent the normal and shear components of displacement discontinuities, respectively. Based on the general concept of linear elastic fracture mechanics (LEFM), the formulations for K_I and K_{II} are given as [51, 52]:

$$K_I = \frac{\mu}{4(1-\nu)} \left(\frac{2\pi}{c}\right)^{1/2} D_y(\mathrm{c})$$
$$K_{II} = \frac{\mu}{4(1-\nu)} \left(\frac{2\pi}{c}\right)^{1/2} D_x(\mathrm{c}) \quad (2)$$

where μ and ν are the shear modulus and Poisson ratio, respectively, and c is the crack's half-length. Based on the above-mentioned concepts, the problems shown in Figures 1 and 2 have been numerically treated for the five central crack orientations 0°, 15°, 30°, 45°, and 55°.

3.2 Finite element modeling of problem

Finite Element Method (FEM) has already been exploited for solving the rock-like material problems [11]. Moreover, the modified version of FEM called the Extended Finite Element Method (XFEM) has been improved for the analyses of crack problems, and widely used for solving different types of problems in fracture mechanics [53-56].

The crack propagation process in this section has been numerically simulated using the Abaqus software. This computer code is based on XFEM, and is designed as a flexible tool for finite element modeling of most engineering problems (Figure 4b). The main flexibility aspect of XFEM in Abacus is the steps that are used to divide the problem history, which is more convenient for each history phase. For example, in a creeping hold, a dynamic transient or a thermal transient, many classes of stress analysis can be solved with XFEM (Abacus) [57]. Based on the above-mentioned concepts, the problem shown in Figures 1 and 2 has been numerically modeled in all the five central crack orientations 0°, 15°, 30°, 45°, and 55°.

3.3 Discrete element modeling

The numerical simulation of crack analyses in rock-like materials can be accomplished by the versatile Discrete Element Method (DEM) [29, 40, 58]. Also the application of extended DEM for crack growth under uniaxial compression in geo-material is explained, and the numerical results are compared with their experimental counterparts [27].

In this work, the crack analyses in rock-like material samples were conducted by the 2D PFC. The discrete element modeling of the fracturing mechanism in the modelled samples is performed by simulating the samples in the form of particle assemblies [59]. The standard method for assembling a PFC2D model for the solution of the problems related to this research work is fully described in reference [29]. The main aspects of the solution process include the generation of particles for a proper simulation of the material sample, the packing of these particles to form a particle assembly of the modelled specimen, the initialization of isotropic stress conditions within the assembly, removing the floating particles from the assembly, and installing the bonds to make a solidified modeled sample for the simulated geo-material specimen. In this modeling procedure, a contact modelling scheme is adopted to simulate the constitutive equations related to the material behavior (Figure 4c). In the parallel bond model, a set of elastic springs is assumed to be distributed over a rectangular contact plane centered at the contact point. The contact point springs are acting parallel to these bond springs. An assembly of rounded particles are free to move in the shear and normal directions but interacting one another via shear and normal springs. They can also rotate within the particle assembly [60]. A proper value for damping factor was estimated as 0.7 in this numerical simulation procedure. Then the modelled specimens shown in Figures 1 and 2 simulated numerically the rock-like material samples containing central cracks of the five crack inclination angles 0°, 15°, 30°, 45°, and 55°.

4. Results and discussion

Results of the crack analyses as obtained from both the laboratory tests and numerical simulation of the pre-cracked samples of the brittle materials (rock-like specimens) are reported and discussed in this section. Also these results are compared to each other and discussed.

As mentioned earlier, the mechanism of crack extension in the specially prepared pre-cracked specimens was investigated. The uniaxial compressive tests were conducted on these specimens in the laboratory. Figure 5 shows the results of the uniaxial loading of the specimens with the central cracks of different inclinations. It was observed experimentally that by changing the angle of the central crack, the crack initiation and propagation patterns also changed. In the experimental modeling, two different types of induced cracks could be observed in the concrete specimens: wing (primary or tensile) and secondary (shear) cracks. If the inclination angle of the central crack is less than 30°, there are only secondary cracks during the loading. Moreover, by increasing the original crack angle, α (i.e. for $\alpha \geq 30^{\circ}$), the wing crack path moves towards the other side of the crack. Therefore, in this case, the primary wing cracks are more dominant during the failure of rock materials, while the secondary cracks are of less importance [6].

In these experiments, the uniaxial compressive strength (UCS) and the crack propagation patterns for each specimen were measured experimentally. Figure 6 shows the variations in UCS of the specimens in the uniaxial compressive test for different pre-existing crack inclination angles. The intact specimen strength (i.e. specimen without a pre-existing crack) is 23 MPa. As it can be seen in Figure 6, as the crack angle (α) increases, the strength of the specimen also increases. Furthermore, a trend line can be fit to these results, and the relationship between the flaw inclination (tanα) and UCS (in MPa) is obtained as follows:

$$UCS = 2.5882 \tan \alpha + 14.05 \quad (3)$$

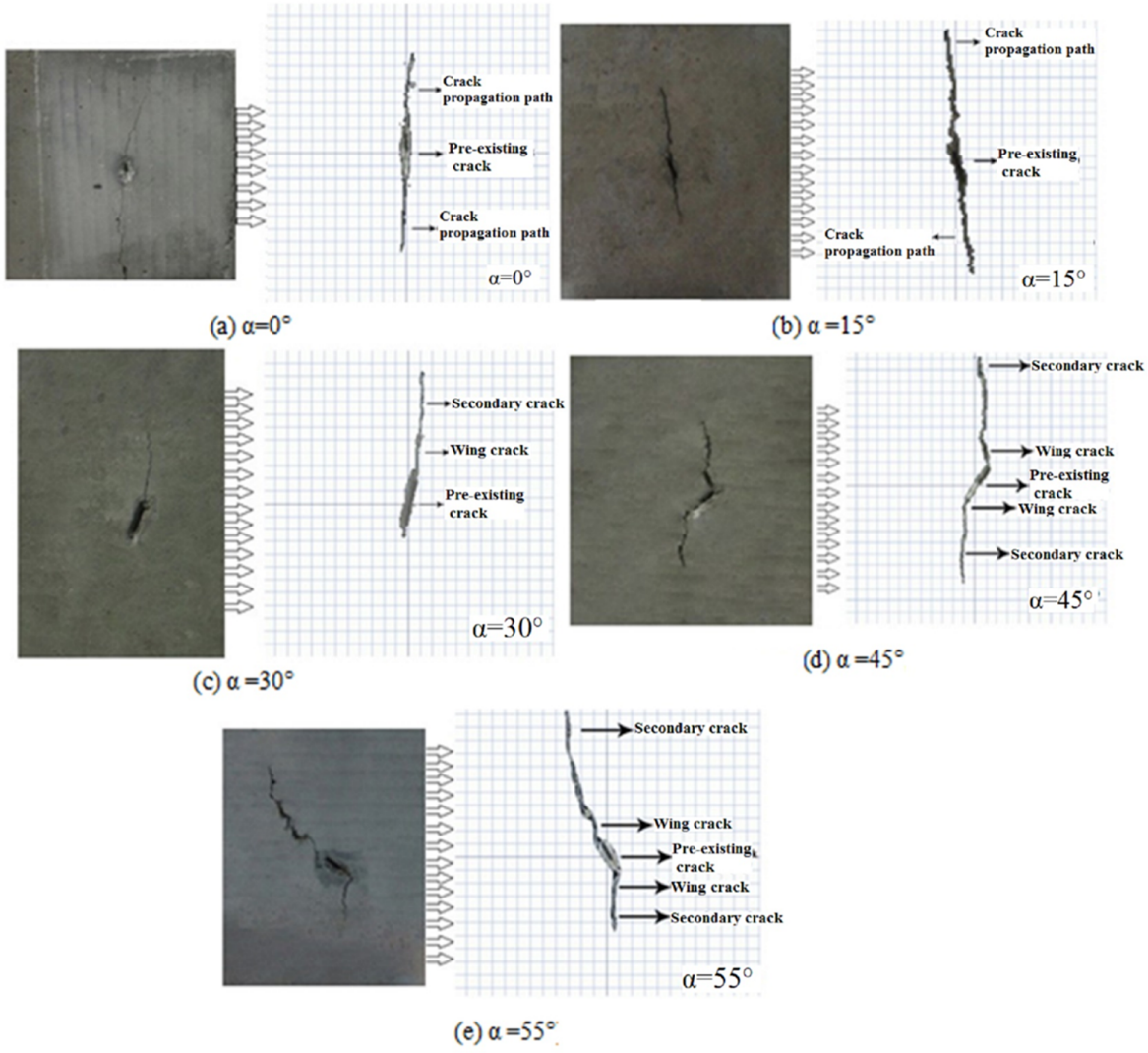

Figure 5: Crack propagation paths observed in experiments for the specimens.

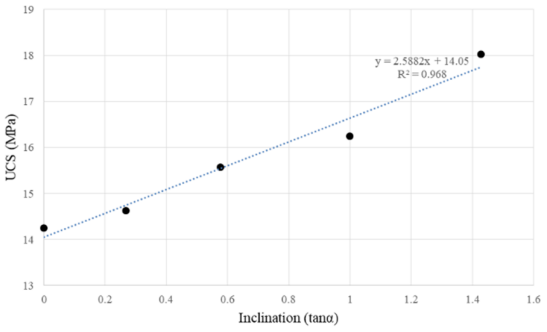

Figure 6: Variations in UCS of the specimens versus inclination of the central crack (*tgα*).

Moreover, crack propagation in the specimens was numerically simulated using BEM. In this case, the specimens were modeled using a 2D displacement discontinuity code (TDDQCR), which was utilized from the quadratic displacement discontinuity elements. The process of crack propagation was simulated under the uniaxial compressive test. The results obtained from modeling of five different specimens are shown in Figure 7. The results of the displacement discontinuity modeling show that if the inclination angle of the central crack is less than 30° ($\alpha < 30^{\circ}$), only the secondary cracks will appear during the uniaxial compressive loading. Moreover, by increasing the central crack angle (for $\alpha \geq 30^{\circ}$), the wing crack path moves towards the other side of the crack. Therefore, in the boundary element modeling (displacement discontinuity modeling), the wing cracks appear for the angles greater than 30° ($\alpha \geq 30^{\circ}$), similar to experimental modeling, and the wing crack propagation is generally agreed with the experimental results. The limitation of TDDQCR is that it is incapable in the simulation of

porosity and grain shape. For the crack angles of less than 30°, the wing cracks are not dominant or may not be observed as they may not get a chance to initiate and propagate. This phenomenon may be related to the crack's tendency, which adjusts its propagation parallel to the direction of the applied compressive loading. The crack tip's shear zone may be formed after the formation of primary cracks due to the stress concentration increase at their tips.

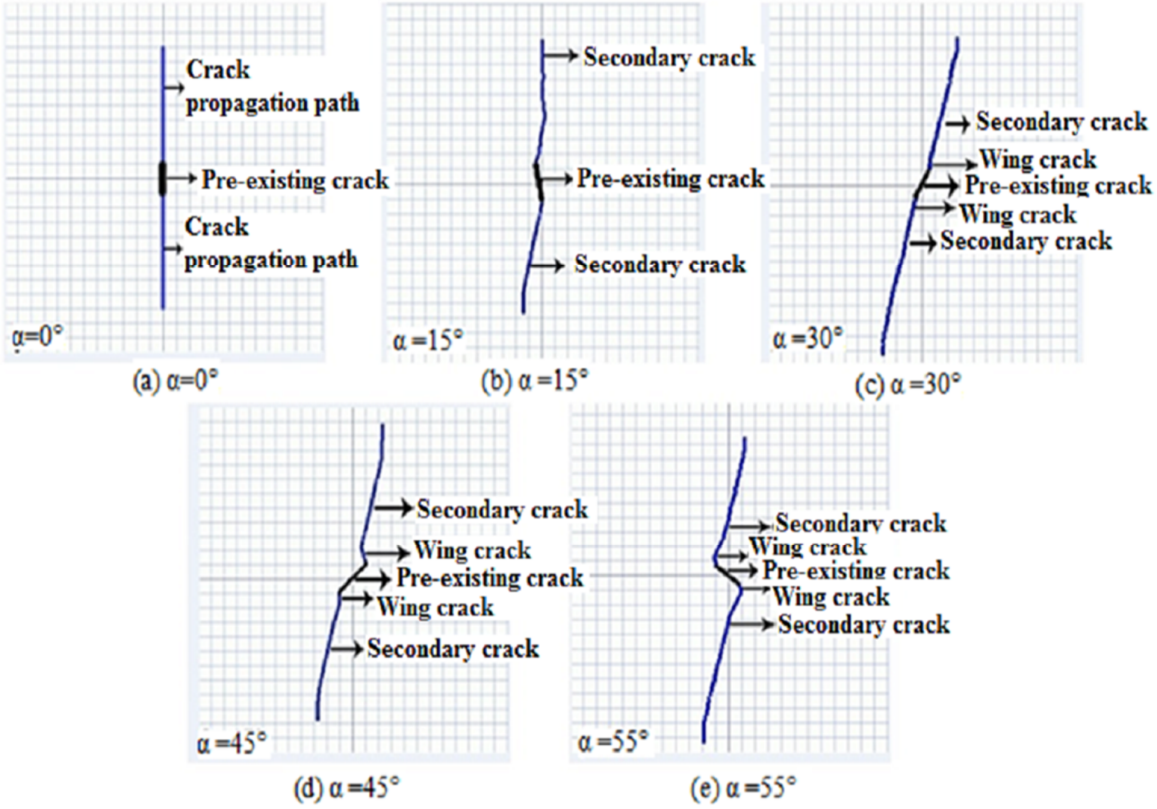

Figure 7: Displacement discontinuity modeling of crack propagation patterns in the modelled specimens with different inclination angles (α) for the pre-existing crack (TDDQCR code).

As mentioned earlier, a finite element modeling was carried out for simulation of the pre-cracked samples. The numerical modelling results of the crack propagation patterns in these five specimens using the Abaqus software are given in Figure 8. In these results, it is shown that if the inclination angle of the central crack is less than 45° ($\alpha < 45^{\circ}$), the secondary cracks are dominant during the uniaxial compressive loading condition. On the other hand, as the inclination angle is greater than 45° ($\alpha \geq 45^{\circ}$), the wing cracks tend to be dominant and replace the secondary cracks. However, the same results were also observed in the physical models for the angles greater than 30° ($\alpha \geq 30^{\circ}$). The limitation of the Abaqus software is that it is incapable in the simulation of porosity and grain shape. In this analysis, when the inclination angles of cracks in the modelled specimens are less than 30°, the observation of wing cracks diminishes, and the secondary or shear cracks appear in the samples. This is mainly due to the tendency of the cracks to propagate parallel to the direction of the applied load. However, the concentration of stresses near the crack tips increases, and the shear zones are produced at their vicinities.

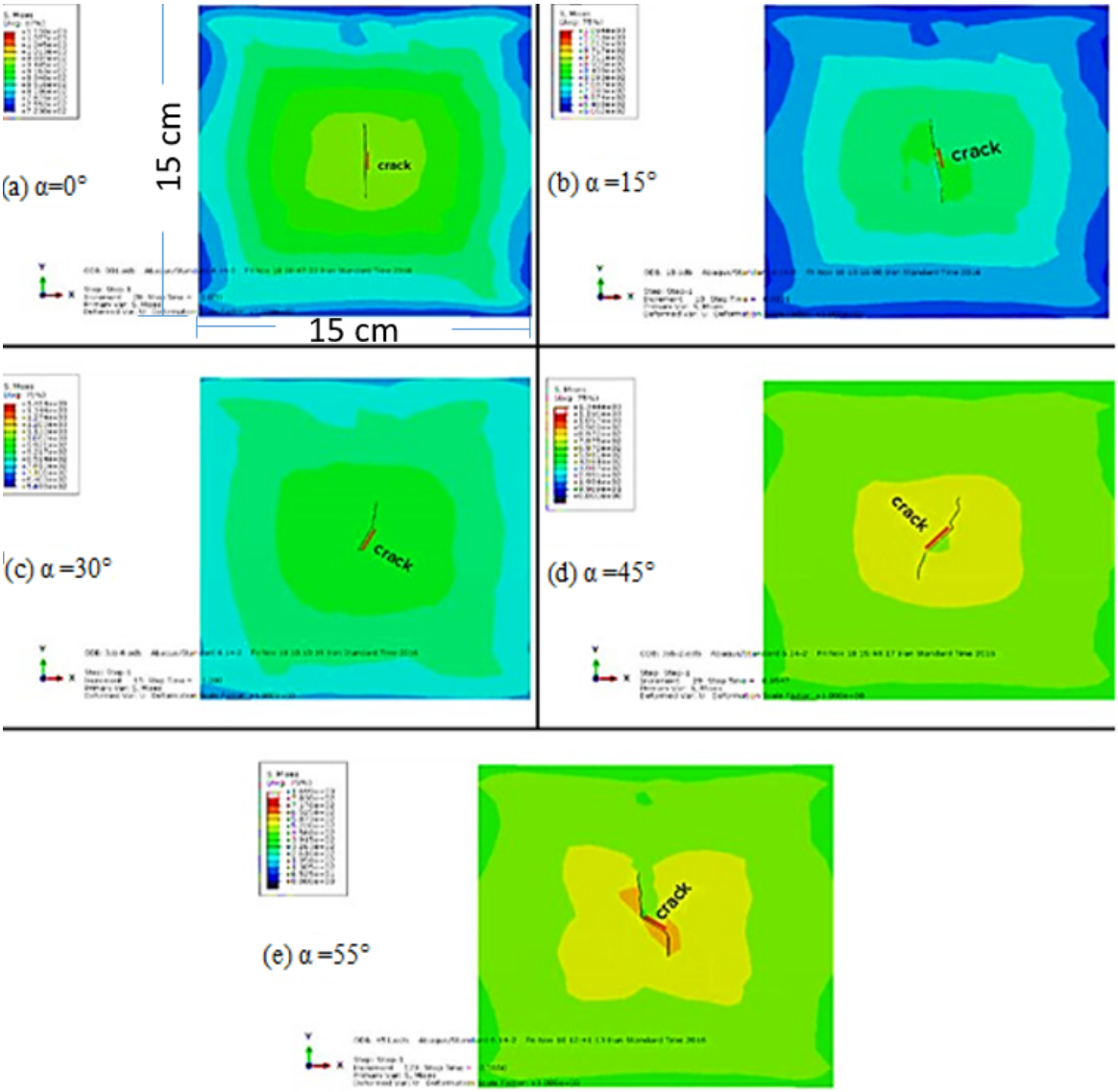

Figure 8: Crack propagation in finite element analyses of the modelled specimens with different angles.

The crack propagation process of the tested samples was also modelled by PFC2D, and the results obtained were shown in Figure 9. In this modeling procedure, the pre-existing cracks of different inclination angles (α) are considered (i.e. $\alpha = 0^{\circ}, 15^{\circ}, 30^{\circ}, 45^{\circ}, 55^{\circ}$). As shown in Figure 9, the simulated crack propagation process by PFC2D is in a good agreement with the corresponding experimental results already given in Figure 5. The results of discrete element modeling also show that for the central crack angle of less than 30° ($\alpha < 30^{\circ}$), only the secondary cracks are visible after the uniaxial compressive loading is applied. Moreover, by increasing the central crack angle (for $\alpha \geq 30^{\circ}$), the wing crack path moves towards the other side of the crack. The main limitations of PFC for crack analyses in geo-materials include: (a) The flaws are closely related to the grain size, and therefore, the grain-size effect should be considered; (b) Some cross-effects may be produced due to the difference between the shape and size of the particles (elements) compared to those of the real grains; (c) It is somewhat difficult to establish a proper relation between the microscopic and macroscopic parameters used in the modelled and physical specimens, respectively, for the geo-material samples.

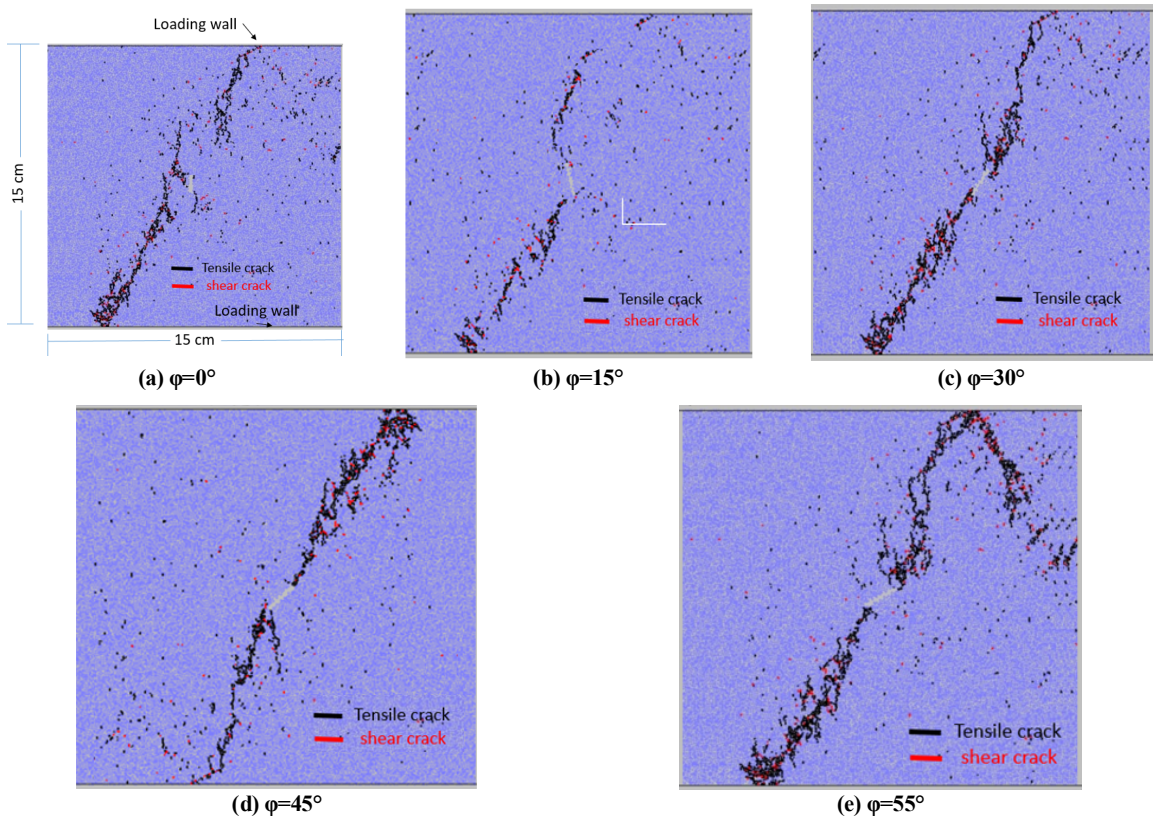

Figure 9: Modelled crack propagation process by DEM for the geo-material specimens containing some pre-existing cracks of different crack inclination angles.

4.1. Calculation of stress intensity factor

The Mode I and Mode II stress intensity factors (SIFs) for the crack tips were calculated using both the analytical and numerical formulations. The analytical formulations to calculate the Mode I and Mode II SIFs (or Mode I and Mode II fracture toughnesses) for the center crack in an infinite space are given as:

$$K_I = \sigma\sqrt{\pi c \varepsilon_I} \tag{4}$$

$$K_{II} = \sigma\sqrt{\pi c \varepsilon_{II}} \tag{5}$$

where K_I and K_{II} are the Mode I and Mode II SIFs, respectively, σ is the compressive stress, c is the half-length of center crack. The two dimensionless coefficients ε_I and ε_{II} are functions of the inclination angle (α), and can be obtained from the following equations:

$$\varepsilon_I = \frac{1 + cos2\alpha}{2} \tag{6}$$

$$\varepsilon_{II} = \frac{sin2\alpha}{2} \tag{7}$$

With more notion in the above equations, it can be understood that SIF is related to the specimen's geometry and crack length.

Moreover, the stress intensity factors are calculated using the DD method, as mentioned earlier in Equation (2). This method has been developed for the analysis of the crack tip element in TDDQCR [42]. However, based on Equation (2) and the analytical Equation (4) and (5), the normalized SIFs, K^N_I and K^N_{II}, are expressed as:

$$sK_I^N = \frac{K_I}{\sigma\sqrt{\pi c}} \tag{8}$$

$$K_{II}^N = \frac{K_{II}}{\sigma\sqrt{\pi c}} \tag{9}$$

The Mode I and Mode II SIFs under the uniaxial compressive test are shown in Figure 10 for both the numerical (using HODDM) and experimental tests. These results obtained show the relatively high accuracy of the numerical values of SIFs as compared to their measured values obtained in the laboratory.

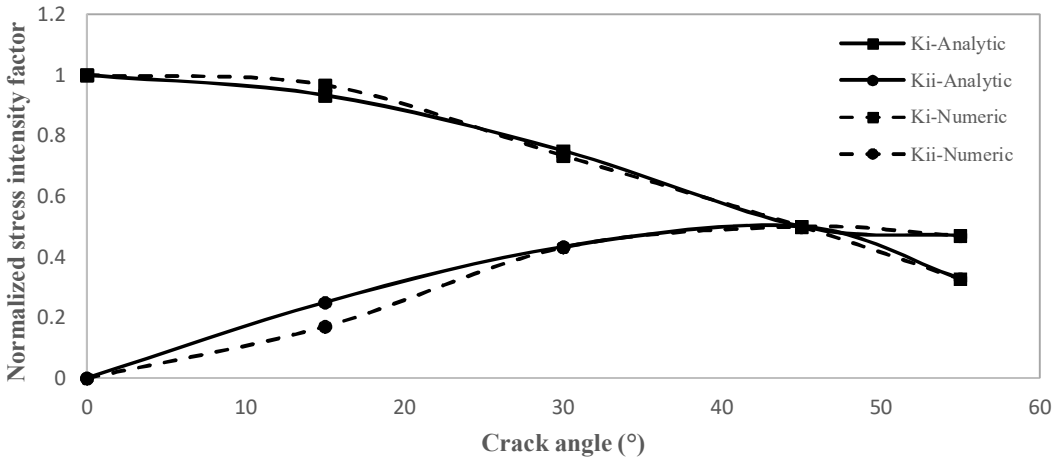

Figure 10: Analytical and numerical values of SIFs considering specimens with different crack inclination angles (α).

5. Conclusions

The effect of the crack inclination angles for a rock-like specimen with central pre-existing crack on the mechanism of crack propagation within the material sample was studied experimentally and numerically. The specially made specimens of rock-like materials containing central cracks with different inclination angles were tested experimentally in the laboratory under the uniaxial loading condition. The crack propagation patterns observed are evident by formation of the wing and shear cracks in the failed specimens. Furthermore, the effect of the inclination angles of the central pre-existing cracks on the wing and secondary cracks propagation paths was studied numerically. For this purpose, some numerical modeling schemes were also performed using DDM (as one of the sub-methods of BEM), FEM, and DEM. Some of the main conclusions of this research work may be given as follow:

- According to the experimental and numerical results, there are two different crack propagation patterns in the specimens as tensile (wing or primary) cracks and shear (secondary).
- If the inclination angle of the central crack is less than 30° ($\alpha < 30^{\circ}$), only the secondary cracks will appear during the uniaxial compressive loading. This is observed in all the experimental and numerical models (except for a small difference in the finite element modeling).
- Based on the results obtained from the experimental and numerical models, by increasing the central crack angle greater than 30° ($\alpha \geq 30^{\circ}$), the wing cracks appear and move towards the other side of the crack (except for a small difference in the finite element modeling).
- The finite element modeling results show that if the central crack's inclination angle is less than 45° ($\alpha < 45^{\circ}$), only the secondary cracks will be observed during the uniaxial compressive loading. Therefore, in the finite element modeling, the wing cracks appear for the angles greater than 45° ($\alpha \geq 45^{\circ}$).
- The results of the experimental and numerical simulations of the crack propagation patterns in the rock-like material samples due to the uniaxial compressive loading conditions are similar to each other. Thus there are good agreements between the experimental and all the three numerical modeling methods.
- In addition to the crack propagation patterns, the uniaxial compressive strength (UCS) for the specimens containing central cracks with various inclination angles was measured. The strength of the pre-cracked specimens increases with increase in the flaw's angle. Furthermore, a relationship between the flaw's angle (α) and UCS was obtained.
- The Mode I and Mode II stress intensity factors (SIFs) were calculated numerically and compared with their corresponding experimentally measured values.

Comparing the results obtained with the

experimental tests, the analytical and numerical methods show that there is a proper agreement between the corresponding analytical and numerical values of SIFs. This confirms the validity of the various methods used in this work and the accuracy of the results obtained herewith.

References

[1]. Bobet, A., Einstein, H.H. (1998). Numerical modeling of fracture coalescence in a model rock material. International Journal of Fracture, 92, 221-252.

[2]. Yaylaci, M. and Avcar, M. (2020). Finite element modeling of contact between an elastic layer and two elastic quarter planes. Computers and Concrete, 26(2), 107-114.

[3]. Yaylaci, M., Bayrak, M.Ç., and Avcar, M. (2019). Finite element modeling of receding contact problem. International Journal of Engineering and Applied Sciences, 11(4), 468-475.

[4]. Yaylaci, M., Terzi, C., and Avcar, M. (2019). Numerical analysis of the receding contact problem of two bonded layers resting on an elastic half plane. Structural Engineering and Mechanics, 72(6), 775-783.

[5]. Zhuang X., Chun J., and Zhu H. (2014). A comparative study on unfilled and filled crack propagations for rock-like brittle materials. Theoretical and Applied Fracture Mechanics, 72, 110-120.

[6]. Zhou X.P., Bi J., and Qian Q.H. (2015). Numerical simulation of crack growth and coalescence in rock-like materials containing multiple pre-existing flaws. Rock Mechanics and Rock Engineering, 48, 1097-1114.

[7]. Wang S.Y., Sloan S.W., Sheng D.C., and Tang C.A. (2016). 3D numerical analysis of crack propagation of heterogeneous notched rock under uniaxial tension. Tectonophysics, 677-678, 45-67.

[8]. Cheng H., Zhou X.P., Zhu J., and Qian Q.H. (2016). The effects of crack openings on crack initiation, propagation and coalescence behavior in rock-like materials under uniaxial compression. Rock Mechanics and Rock Engineering, 49 (9), 3481-3494.

[9]. Wang Y., Zhou X., and Shou Y. (2017). The modeling of crack propagation and coalescence in rocks under uniaxial compression using the novel conjugated bond-based peridynamics. International Journal of Mechanical Sciences, https://doi.org/10.1016/j.ijmecsci.2017.05.019.

[10]. Lak M., Fatehi Marji M., Yarahmadi A., and Abdollahipour A. (2019). A coupled finite difference-boundary element method for modeling the propagation of explosion-induced radial cracks around a wellbore. Journal of Natural Gas Science and Engineering, 64, 41-51.

[11]. Wang H., Dyskin A., Pasternak E., Dight Ph., and Sarmadivaleh M. (2019). Experimental and Numerical Study of 3D Crack Growth from a Spherical Pore in Biaxial Compression. Rock Mechanics and Rock Engineering, https://doi.org/10.1007/s00603-019-01899-1.

[12]. Wang M., Wan W., and Zhao W. (2020). Experimental study on crack propagation and the coalescence of rock-like materials with two pre-existing fissures under biaxial compression. Bulletin of Engineering Geology and the Environment, https://doi.org/10.1007/s10064-020-01759-1.

[13]. Bi J., Zhou X.P., and Qian Q.H. (2016). The 3D numerical simulation for the propagation process of multiple pre-existing flaws in rock-like materials subjected to biaxial compressive loads. Rock Mechanics and Rock Engineering, 49, 1611-1627.

[14]. Huang Sh., Yao N., Ye Y., and Cui X. (2019). Strength and failure characteristics of rock-like materials containing a large-opening crack under uniaxial compression: experimental and numerical studies. International Journal of Geo-mechanics 19 (8).

[15]. Zhuang X., Chun J., and Zhu H. (2014). A comparative study on unfilled and filled crack propagation for rock-like brittle material. Theoretical and Applied Fracture Mechanics, 72, 110-120.

[16] Zhou X.P., Bi J., and Qian Q.H. (2015). Numerical simulation of crack growth and coalescence in rock-like materials containing multiple pre-existing flaws. Rock Mechanics and Rock Engineering, 48, 1097-1114.

[17]. Uzun Yaylacı, E., Yaylacı, M., Ölmez, H., and Birinci, A., (2020). Artificial Neural Network Calculations for a Receding Contact Problem, Computers and Concrete, Vol. 25, 6, https://doi.org/10.12989/cac.2020.25.6.000.

[18]. Wang S.Y., Sloan S.W., Sheng D.C., and Tang C.A. (2016). 3D numerical analysis of crack propagation of heterogeneous notched rock under uniaxial tension. Tectonophysics, 677-678, 45-67.

[19]. Cao, S., Yilmaz, E., Xue, G.L., and Song, W.D., (2019). Assessment of acoustic emission and triaxial mechanical properties of rock-cemented tailings matrix composites. Advances in Materials Science and Engineering, Article 6742392, https://doi.org/10.1155/2019/6742392.

[20]. Yan, B., Lai, X., Jia, H., Yilmaz, E., and Hou, C. (2021). A solution to the time-dependent stress distribution in suborbicular backfilled stope interaction with creeping rock. Advances in Civil Engineering, Article ID 5533980, https://doi.org/10.1155/2021/5533980.

[21]. Cao R.H., Cao P., Lin H., Ma G.W., Fan X., and Xiong X.G. (2018). Mechanical behavior of an opening in a jointed rock-like specimen under uniaxial loading: Experimental studies and particle mechanics approach. Archives of Civil and Mechanical Engineering 18

(1):198-214.

[22]. Yaylacı, M., Eyüboğlu, A., Adıyaman, G., Uzun Yaylacı, E., Öner, E., and Birinci, A. (2021). Assessment of different solution methods for receding contact problems in functionally graded layered mediums, Mechanics of Materials, https://doi.org/10.1016/j.mechmat.2020.103730.

[23]. Zhao Zh., Jing H., Shi X., and Han G. (2019). Experimental and numerical study on mechanical and fracture behavior of rock-like specimens containing pre-existing holes flaws. European Journal of Environmental and Civil Engineering, https://doi.org/10.1080/19648189.2019.1657961.

[24]. Wu T., Gao Y., Zhou Y., and Li J. (2020). Experimental and numerical study on the interaction between holes and fissures in rock-like materials under uniaxial compression. Theoretical and Applied Fracture Mechanics, https://doi.org/10.1016/j.tafmec.2020.102488.

[25]. Sun X.Z., Wang H.L., Liu K.M., Zhan X.C., and Jia C.Y. (2019). Experimental and numerical studies on mixed crack propagation characteristics in rock-like materials under uniaxial loading. Geotechnical and Geological Engineering, https://doi.org/10.1007/s10706-019-01007-8.

[26]. Hosseini-Nasab H. and Fatehi Marji M. (2007). A semi-infinite higher-order displacement discontinuity method and its application to the quasi-static analysis of radial cracks produced by blasting. Journal of Mechanics of Materials and Structures, 2 (3), 439-458.

[27]. Yang L., Jiang Y., Li B., Li S., and Gao Y. (2012). Application of the expanded distinct element method for the study of crack growth in rock-like materials under uniaxial compression. Frontiers of Structural and Civil Engineering, 6 (2), 121-131.

[28]. Jaya B.N., Kirchlechner C., and Dehm G. (2015). Can microscale fracture tests provide reliable fracture toughness values? A case study in silicon. Journal of Materials Research, 30 (5), 686-698.

[29]. Lecrec W., Haddad H., and Guessasma M. (2017). On the suitability of a Discrete Element Method to simulate cracks initiation and propagation in heterogeneous media. International Journal of Solids and Structures, 118, 98-114.

[30]. Zhang P., Du Sh., Brik C., and Zhao W. (2019). A scaled boundary finite element method for modelling wing crack propagation problems. Engineering Fracture Mechanics, 216.

[31]. Yaylacı M., Adıyaman E., Öner E., and Birinci A. (2021). Investigation of continuous and discontinuous contact cases in the contact mechanics of graded materials using analytical method and FEM, Computers and Concrete. 27(3),199-210.

[32]. Zhang X.P. and Wong L.N.Y. (2013). Crack initiation, propagation and coalescence in rock-like materials containing two flaws: a numerical study based on bonded-particle model approach. Rock Mechanics and Rock Engineering, 46, 1001-1021.

[33]. Wang M., Zheming Z., and Jun X. (2015). Experimental and numerical studies of the mixed-mode Ⅰ and Ⅱ crack propagation under dynamic loading using SHPB. Chinese Journal of Rock Mechanics and Engineering, 12.

[34]. Ai D., Zhao Y., Wang Q., and Li Ch. (2019). Experimental and numerical investigation of crack propagation and dynamic properties of rock in SHPB indirect tension test. International Journal of Impact Engineering, 126, 135-146.

[35]. Zhou S.W. and Xia C.C. (2018). Propagation and coalescence of quasi-static cracks in Brazilian disks: an insight from a phase field model. Acta Geotechnica. https://doi.org/10.1007/s11440-018-0701-2.

[36]. Kou M.M., Lian Y.J., and Wang Y.T. (2019). Numerical investigations on crack propagation and crack branching in brittle solids under dynamic loading using bond-particle model. Engineering Fracture Mechanics, 212, 41-56.

[37]. Trivino L.F. and Mohanty B. (2015). Assessment of crack initiation and propagation in rock from explosion-induced stress waves and gas expansion by cross-hole seismometry and FEM–DEM method. International Journal of Rock Mechanics and Mining Sciences, 77, 287-299.

[38]. Lak M., Fatehi Marji M., and Yarahamdi Bafghi A. (2018). A finite difference modelling of crack initiation in rock blasting. The 2018 World Congress on Advances in Civil, Environmental, and Materials Research (ACEM18), Songdo Convensia, Incheon, Korea.

[39]. He Ch. and Yang J. (2019). Experimental and numerical investigations of dynamic failure process in rock under blast loading. Tunneling and Underground Space Technology, 83, 552-564.

[40]. Crouch S.L. and Starfield A.M., Boundary Element Methods in Solid Mechanics, George Allen and Unwin, London, 1983. Ping Y., Li S.C. (2014). Particle discrete method based on manifold cover for crack propagation of jointed rock mass. Mathematical Problems in Engineering, https://doi.org/10.1155/2014/315983.

[41]. Yaylaci Murat (2016). The investigation crack problem through numerical analysis. Structural Engineering and Mechanics, 57(6), 1143-1156., Doi: 10.12989/sem.2016.57.6.1143.

[42]. Fatehi Marji M. (1997). Modeling of cracks in rock fragmentation with a higher order Displacement Discontinuity Method. Dissertation, PhD Thesis in rock mechanics. Mining Engineering Department, Middle East Technical University (METU), Ankara, Turkey.

[43]. Fatehi Marji M., Hosseini_Nasab H., and Kohsary A.H. (2007). A new cubic element formulation of the

displacement discontinuity method using three special crack tip elements for crack analysis, JP J. Solids Struct., 1 (1), 61-91.

[44]. Yaylacı, M., Adıyaman, E., Öner, E., and Birinci, A., (2020). Examination of analytical and finite element solutions regarding contact of a functionally graded layer, Structural Engineering and Mechanics. 44,54-67.

[45]. Fatehi Marji M., Hosseini-Nasab H., and Morshedi A. (2009). Numerical modeling of crack propagation in rocks under TBM disc cutters. Journal of Mechanics of Materials and Structures, 4 (3), 605-627.

[46]. Behnia M., Goshtasbi K., Fatehi Marji M., and Golshani A. (2011). On the crack propagation modeling of hydraulic fracturing by a hybridized displacement discontinuity/boundary collocation method, Journal of Mining and Environment 2 (1), 1-16.

[47]. Haeri H., Shahriar K., Fatehi Marji M., and Moarefvand P. (2015). A coupled numerical-experimental study of the breakage process of brittle substances. Arabian Journal of Geosciences, 8, 809-825.

[48]. Fatehi Marji M. (2015). Simulating the crack coalescence mechanism underneath the single and double disc cutters by a higher order displacement discontinuity method. Journal of central south university, 22 (3), 1045-1054.

[49]. Fatehi Marji M., Hosseini_Nasab H., and Kohsary A.H. (2006). On the Uses of Special Crack Tip Elements in Numerical Rock Fracture Mechanics. International Journal of Solids and Structures, 43, 1669-1692.[50]. Fatehi Marji M. (1990). Crack propagation modeling in rocks and its application to indentation problems, MSc. Thesis in rock mechanics, Mining Engineering Department, Middle East Technical University (METU), Ankara, Turkey.

[51]. Yaylaci Murat and Birinci Ahmet (2013). The receding contact problem of two elastic layers supported by two elastic quarter planes. Structural Engineering and Mechanics, 48(2), 241-255., Doi: 10.12989/sem.2013.48.2.241.

[52]. Öner Erdal, Yaylaci Murat, and Birinci Ahmet (2015). Analytical solution of a contact problem and comparison with the results from FEM. Structural Engineering and Mechanics, 54(4), 607-622., Doi: 10.12989/sem.2015.54.4.00.[53]. Adiyaman G, Yaylacı M., and Birinci A. (2015). Analytical and finite element solution of a receding contact problem. Structural Engineering and Mechanics, 54(1), 69-85., Doi: 10.12989/sem.2015.54.1.069.

[54]. Asareh I. and Song J.H. (2019). Nonnodal Extended Finite-Element Method for Crack Modeling with Four-Node Quadrilateral Elements. Journal of Engineering Mechanics, 145 (10).[55]. Jiang Z. and Xiang J. (2020). Method using XFEM and SVR to predict the fatigue life of plate-like structures. Structural Engineering and Mechanics, 73 (4), 455-462.

[56]. Abaqus (2011). GUI. User's Manual 6.11. Dassault Systems Simulia Corp, Providence, Rhode Island, USA.

[57]. Fabjan T., Ivars D.M., Vukadin V. (2015). Numerical simulation of intact rock behaviour via the continuum and Voronoi tesselletion models–a sensitivity analysis. Acta Geotechnica Slovenica, 12 (2), 4-24.

[58]. Cundall P.A. and Strack O.D.L. (1979). A discrete numerical model for granular assemblies. Geo-technique 29:47-65.

[59]. Wang T., Zhou W., Chen J., Xiao X., Li Y., and Zhao X. (2014). Simulation of hydraulic fracturing using particle flow method and application in a coal mine. International Journal of Coal Geology, 121, 1-13.

[60]. Wong L.N.Y. and Einstein H. (2006). Fracturing behavior of prismatic specimens containing single flaws. 41st U.S. Symposium on Rock Mechanics, Colorado.

تجزیه و تحلیل شکست فشاری مواد شبه سنگی با استفاده از روش های آزمایشگاهی و عددی

محمد داوود یاوری[۱]، هادی حائری[۲]، وهاب سرفرازی[۳]، محمد فاتحی مرجی[۴*] و حسینعلی لازمی[۱]

۱- بخش مهندسی معدن ، دانشگاه آزاد اسلامی واحد بافق، بافق ، ایران

۲-آزمایشگاه اصلی دولتی برای ژئومکانیک عمیق و مهندسی زیرزمین، پکن، چین

۳- بخش مهندسی معدن، دانشگاه صنعتی همدان، همدان، ایران

۴-بخش مهندسی استخراج معدن، دانشکده معدن و متالورژی، دانشگاه یزد، یزد ، ایران

ارسال ۲۰۲۱/۰۵/۰۹، پذیرش ۲۰۲۱/۰۶/۰۳

* نویسنده مسئول مکاتبات: mohammad.fatehi@gmail.com

چکیده:

بررسی مکانیزم انتشار ترک از اهمیت بالایی در تحلیل فرایند شکست بیشتر مواد برخوردار است. این فرآیند ممکن است در هنگام بارگذاری هر نوع مواد در معرض آن قرار گیرد. در این تحقیق، مکانیسم ترک خوردگی در مواد شبه سنگ با استفاده از روش‌های عددی بررسی شده و با نتایج آزمایشگاهی مقایسه می‌شود. با این حال، مکانیسم رشد ترک در مواد شکننده همانند سنگ تحت تأثیر پارامترهای مختلف است. این کار تحقیقاتی بر تأثیر زاویه‌های ترک اولیه در مسیر رشد ترک این مواد متمرکز است. برخی از نمونه‌های مکعبی حاوی ترک‌های از پیش موجود با در نظر گرفتن جهت‌داری‌های مختلف تحت بارگذاری فشاری آزمایش می‌شوند. نمونه‌ها از سیمان، آب، شن و ماسه ساخته شده‌اند. علاوه بر این، فرآیند ذکر شده با استفاده از سه روش مختلف از نظر عددی شبیه سازی شده است: روش المان محدود برای اجسام ناپیوسته، روش المان مجزا و روش ناپیوستگی جابجایی. پارامترهای میکرو برای شبیه‌سازی با روش آزمون و خطا برای روش المان مجزا بدست می‌آیند. در نهایت، مسیرهای رشد ترک مشاهده شده در مدل‌های آزمایشگاهی با مدل‌های شبیه سازی شده عددی مقایسه می‌شود. نتایج به دست آمده نشان می‌دهد که این ترک‌های مرکزی به دو روش منتشر می شوند که به زاویه اولیه آنها بستگی دارد. با افزایش زاویه ترک اولیه به بیشتر از ۳۰ درجه ($\alpha>30$)، مسیر ترک کششی بیشتر از ترک اولیه فاصله می‌گیرد و با کاهش α به کوچکتر از ۳۰ درجه ($\alpha<30$)، فقط ترک‌های برشی شروع شده‌اند. بنابراین، اعتبار و صحت نتایج با مقایسه تمام نتایج متناظر با روشهای مختلف آشکار می‌شود. بر اساس این نتایج، به طور کلی می‌توان نتیجه گرفت که مقاومت نمونه‌های مکعبی (مواد سنگی) با افزایش در زاویه‌های ترک با توجه به جهت بارگذاری اعمال شده، افزایش می‌یابد .

کلمات کلیدی: مکانیزم ترک خوردگی، مکانیک شکست؛ نمونه مکعبی، مدل سازی فیزیکی، FEM، DEM.